Dielectric functions and optical constants modeling for CuIn3Se5 and CuIn5Se8

M. León, R. Serna, S. Levcenko, A. Nicorici, J. M. Merino et al.

Citation: J. Appl. Phys. **103**, 103503 (2008); doi: 10.1063/1.2921865
View online: http://dx.doi.org/10.1063/1.2921865
View Table of Contents: http://jap.aip.org/resource/1/JAPIAU/v103/i10
Published by the American Institute of Physics.

Dielectric functions and optical constants modeling for $CuIn_3Se_5$ and $CuIn_5Se_8$

M. León,[1] R. Serna,[2] S. Levcenko,[3] A. Nicorici,[3] J. M. Merino,[1] E. J. Friedrich,[1] and E. Arushanov[1]
[1]*Departamento de Física Aplicada, Universidad Autónoma de Madrid, C-XII, 28049 Madrid, Spain*
[2]*Instituto de Óptica, CSIC, Serrano 121, 28006 Madrid, Spain*
[3]*Institute of Applied Physics, Academy of Sciences of Moldova, Chisinau MD 2028, Moldova*

(Received 22 October 2007; accepted 13 March 2008; published online 16 May 2008)

The complex dielectric functions, $\varepsilon(\omega)=\varepsilon_1(\omega)+i\varepsilon_2(\omega)$, of $CuIn_3Se_5$ and $CuIn_5Se_8$ crystals with different Cu contents have been determined in the 0.8–4.7 eV photon energy range by using spectroscopic ellipsometry. The spectral dependence of the real, $\varepsilon_1(\omega)$, and imaginary, $\varepsilon_2(\omega)$, parts of $\varepsilon(\omega)$, as well as the complex refractive index, the absorption coefficient, and the normal-incidence reflectivity, has been modeled by using a modification of Adachi's model. The results are in excellent agreement with the experimental data over the entire range of photon energies. The model parameters, including the energies corresponding to the lowest direct gap, E_0, and to higher critical points, have been determined by using the simulated annealing algorithm.
 [DOI: 10.1063/1.2921865]

I. INTRODUCTION

$CuInSe_2$ and related chalcopyrite-type semiconductors are leading candidates as absorbers in high-efficiency heterojunction solar cells. Devices based on $CuIn_{1-x}Ga_xSe_2$ have demonstrated efficiencies up to 19.3%.[1] Several studies showed the existence of an ordered-defect-compound (ODC) surface layer, with stoichiometries close to that of $CuIn_3Se_5$, on the $CuInSe_2$ absorber in some high-efficiency thin film cells. This surface layer is expected to play an important role in the performance of high-efficiency $CuIn_{1-x}Ga_xSe_2$-based solar cells.[2–4] Therefore, a detailed study of the physical properties of $CuIn_3Se_5$ and $CuIn_5Se_8$ ODCs seems to be essential to control such performance; so far their characteristics have not yet been well determined. Some optical measurements were carried out in $CuIn_3Se_5$ (Refs. 4–8) and $CuIn_5Se_8$ (Refs. 8–14) both thin films and bulk samples and the band gap values E_g were estimated.

Spectroscopic ellipsometry is a nondestructive and powerful technique to investigate the optical response of semiconductors. This response is determined by the frequency-dependent complex dielectric function and, in addition, the main features of the band structure, such as interband transitions, can be derived from the analysis of the complex dielectric function and its derivatives.

Recently, Han *et al.*[14] reported the optical functions of thin polycrystalline $(4CuInSe_2)_y(CuIn_5Se_8)_{1-y}$ films with different Cu contents derived from spectroscopic ellipsometry measurements. In the same work, the authors described the changes in the optical functions with the Cu-deficiency degree. However, among the studied films, no compositions close to $CuIn_3Se_5$ (Cu: 11.11 at. %) or $CuIn_5Se_8$ (Cu: 7.14 at. %) were included.

In the present study, the complex dielectric function spectra of several samples with different deviations from the $CuIn_3Se_5$ and $CuIn_5Se_8$ stoichiometries have been measured by spectroscopic ellipsometry at room temperature and their optical constants have been modeled. A comparison of the optical properties between nearly stoichiometric and Cu-poor crystals has also been performed.

II. EXPERIMENTAL METHODS AND ANALYSIS METHODOLOGY

$CuIn_3Se_5$ and $CuIn_5Se_8$ crystals were grown by the Bridgman method. Energy dispersive x-ray microanalysis (EDAX) was used to measure the composition of the samples. The results of such analysis are shown in Table I. For each nominal composition, two kinds of samples were used in the optical study: the nearly stoichiometric samples, I35S and I58S (Table I), and the samples showing some deviations from the nominal composition, I35N and I58N (Table I). The structural analysis was performed by x-ray diffraction and it was found that the ingots of I35 and I58 were of polycrystalline single phase, which presents tetragonal and hexagonal structures, respectively.

The optical measurements were performed at room temperature in the photon energy range from 0.8 to 4.7 eV at two incidence angles Φ, 55° and 65°, by using a variable-angle spectroscopic ellipsometer.[15] In order to remove the surface undesired overlayers, the samples were prepared as described in Ref. 16 and, hence, a two phase model (atmosphere-sample) was used to analyze the ellipsometry spectra. The complex dielectric functions have been determined as follows:[16,17]

TABLE I. Compositional data of the samples resulting from EDAX.

Samples	Cu (at. %)	In (at. %)	Se (at. %)	In/Cu	Se/Cu
$CuIn_3Se_5$(I35S)	11.2	30.9	57.9	2.8	5.2
$CuIn_3Se_5$(I35N)	9.5	31.4	59.1	3.3	6.2
$CuIn_5Se_8$(I58S)	7.1	32.8	60.1	4.6	8.5
$CuIn_5Se_8$(I58N)	6.5	33.1	60.4	5.1	9.3

$$\varepsilon = \sin^2\Phi\left[1+\tan^2\Phi\left(\frac{1-\rho}{1+\rho}\right)^2\right], \quad (1)$$

where $\rho=r_p/r_s$ is the complex reflectance ratio, and r_p and r_s refer to the electric field reflection coefficients for parallel (p) and perpendicular (s) polarizations of the light beam defined with respect to the incidence plane.

The features observed in the complex dielectric function spectra $\varepsilon=\varepsilon(\hbar\omega)$ of a semiconductor are related to interband transitions originated by large or singular values of the joint valence and conduction density of states (DOS). In order to analyze in detail the observed structure of the $\varepsilon=\varepsilon(\hbar\omega)$ spectra, a modification of Adachi's model has been used in this work. This model combines the merit of the standard critical point (CP) and damped harmonic oscillator models[18] and it has been successfully applied to model the dielectric functions of several III-V, I-III-VI_2, and ODC compounds as well as their optical constants.[19–23] In this model, which has also been extensively explained in a previous work,[23] the complex dielectric function is described as a function of energy, $E=\hbar\omega$ by the sum of two terms, $\varepsilon_0(E)$ and $\varepsilon_1(E)$, which correspond respectively to the one-electron contributions at the $E_{0\alpha}$ and $E_{1\beta}$ CPs, where $\alpha=a,b,c$ refers to the triple valence band (VB) splitting level in chalcopyrites, and $\beta=A,B$ refers to different energy transitions after the main one. It is worth mentioning that, in our case, the triple VB splitting at the E_0 CPs has not been observed and has been treated as a single degenerate one. Following after Djurisic and co-workers[21,22] in the case of the E_{1A} transition model, the damping constant Γ has been replaced by the frequency-dependent damping constant.[23] The replacement permits us to get a better agreement between the calculated and the experimental data.

On the other hand, the simulated annealing (SA) algorithm has been used to obtain Adachi's model parameters through the minimization of the following objective function:[21,22,24]

$$F=\sum_{i=1}^{N}\left(\left|\frac{\varepsilon_1(\omega_i)}{\varepsilon_1^{\text{expt}}(\omega_i)}-1\right|+\left|\frac{\varepsilon_2(\omega_i)}{\varepsilon_2^{\text{expt}}(\omega_i)}-1\right|\right)^2, \quad (2)$$

where the summation is performed over the available range of experimental points, and $\varepsilon_1^{\text{expt}}(\omega_i)$, $\varepsilon_1(\omega_i)$, $\varepsilon_2^{\text{expt}}(\omega_i)$, and $\varepsilon_2(\omega_i)$ are the experimental and calculated values, respectively, of the real and imaginary parts of the complex dielectric function at the ω_i point. Such algorithm has shown good agreement with the experimental data for III-V materials and ODC compounds.[19–23]

III. RESULTS AND DISCUSSIONS

Figures 1(a) and 1(b) show the real $\varepsilon_1(\omega)$ and imaginary $\varepsilon_2(\omega)$ parts of the pseudodielectric function $\varepsilon(\omega)=\varepsilon_1(\omega)+i\varepsilon_2(\omega)$ for I35 and I58 samples, respectively. The spectra exhibit several CP structures and so Adachi's model has been applied to calculate the dielectric function and the optical constants of the studied crystals. The resulting analytical lines from the fits of the experimental data in Fig. 1 have been obtained considering three-dimensional-type CPs in the E_g region and two-dimensional type in the E_1 region. The A, B, E, and Γ model parameters calculated by using the SA algorithm are included in Table II. The lowest E value observed in the region below 1.5 eV corresponds to the fundamental energy gap value, $E_0=E_g$, well distinguished for each studied sample (Fig. 1). A second, E_{1A}, and a third, E_{1B}, energy threshold appear in the region between 2.5 and 4.5 eV (Table II). An excellent agreement between our calculations and the experimental data can be observed for both nearly stoichiometric crystals and also for those with stoichiometric deviations [Figs. 1(a) and 1(b)]. As an indication of the accuracy with respect to the experimental values, the relative errors have been calculated, lying in the 1%–2.3% and 2.4%–5.2% ranges for the real and imaginary parts, respectively, for the studied compounds (Table II). In order to compare with the standard method, the values of E_0 and E_1 have been calculated by fitting the numerically differentiated experimental spectrum to analytical line shapes and are shown in Table II. A good agreement with the values calculated by using the SA algorithm can be observed.

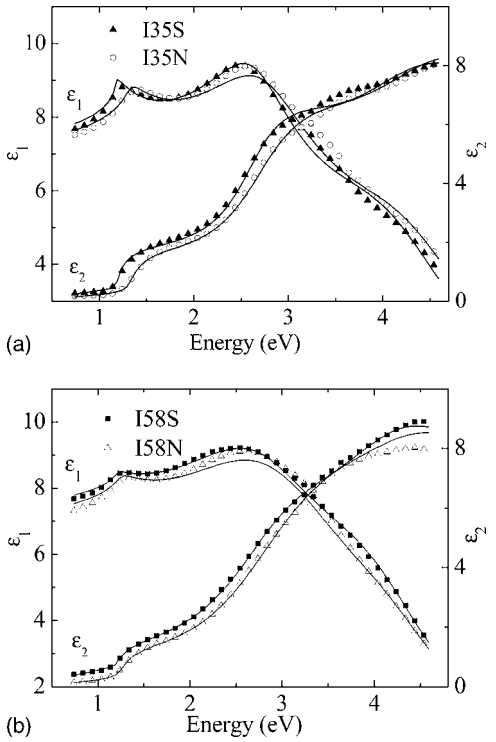

FIG. 1. Real (ε_1) and imaginary (ε_2) parts of the dielectric function vs energy for (a) I35 and (b) I58 samples. Experimental data (triangles, circles, and squares) and fits of these data to Adachi's model using Eq. (2) (solid lines) are also presented.

Since band structure calculations are not available for $CuIn_3Se_5$ and $CuIn_5Se_8$ compounds, the ones obtained for $CuInSe_2$ (CIS) (Ref. 25) and $(4CuInSe_2)_y(CuIn_5Se_8)_{1-y}$ (Ref. 14) have been used to identify the observed energy values. It is well established that the main transitions contributing to $\varepsilon(E)$ in $CuInSe_2$ occur at the Brillouin zone (BZ) center, Γ, and at the BZ edge points, N and T (predominant upper transitions).[16] As mentioned above, the energy threshold of the fundamental absorption edge, $E_0=E_g$, can be well identified in the I35 and I58 spectra [Figs. 1(a) and 1(b)] and can be related to an electronic transition at the Γ point, corresponding to a direct transition from the VB maximum

TABLE II. Model parameter values.

Parameters	Samples							
	I35S		I35N		I58S		I58N	
A (eV$^{1.5}$)	4.20		5.77		2.27		3.63	
E_0 (eV)	1.18 (1.19)[a]		1.32 (1.32)		1.21 (1.20)		1.24 (1.25)	
Γ (eV)	0.005		0.033		0.015		0.045	
B_{1A} (eV)	2.95		2.51		3.83		3.60	
E_{1A} (eV)	2.63 (2.57)		2.72 (2.64)		2.72 (2.70)		2.85 (2.77)	
Γ_{1A} (eV)	0.41		0.39		0.66		0.60	
α	0.03		0.14				0.17	
B_{1B} (eV)	3.92		4.01		3.47		3.07	
E_{1B} (eV)	4.13		4.23		3.95		4.19	
Γ_{1B} (eV)	0.87		0.80		0.71		0.76	
Error	ε_1	ε_2	ε_1	ε_2	ε_1	ε_2	ε_1	ε_2
	2.2%	4.2%	2.2%	5.2%	1%	2.4%	2.3%	3.0%

[a]Values of E_0 and E_1 calculated by fitting the numerically differentiated experimental spectrum to analytical line shapes are in brackets.

(VBM) to the conduction band minimum (CBM). The deduced values of E_g at room temperature, 1.18–1.32 eV for I35 and 1.21–1.24 eV for I58 (Table II), are in reasonable agreement with those[4–14] previously determined by using optical absorption spectra data as well as with the theoretically calculated value of $E_g=1.34-1.35$ eV for I58.[26]

In the region between 2.5 and 4.5 eV, two transitions, named E_{1A} and E_{1B}, have been observed for all I35 and I58 samples. We have assumed that they can be related to N type transitions after Refs. 16 and 27, where ellipsometric data for $CuInSe_2$ were analyzed. The measured energy gap between these two transitions corresponds to the crystal-field splitting of the valence band at the N point in the BZ and, hence, in the present work, the crystal-field splitting at the N point was found to be about 1.5 and 1.3 eV for the I35 and I58 samples, respectively, close to that (1.2–1.3 eV) estimated for $CuGa_3Se_5$[23] and $CuGa_5Se_8$.[28] A value at around 0.8 eV was reported for $CuGa_xIn_{i-x}Se_2(0\leq x\leq 1)$ alloys.[16,19,27]

On the other hand, the variation in the observed band gap values of the presently studied samples can be attributed to compositional changes in the ODC materials. As a matter of fact, the effect of Cu deficiency on the optical functions of $CuInSe_2$, $(4CuInSe_2)_y(CuIn_5Se_8)_{1-y}$, and $CuIn_{1-x}Ga_xSe_2$ (CIGS) thin films was recently reported and discussed.[14,29,30] In those works, a reduction in the absorption strength in the spectral region between 1 and 3 eV for Cu-poor samples was found, and it was explained in terms of the Cu 3d states DOS. Cu-poor CIS and CIGS materials show an increase in the band gap due to the reduction in repulsion between the Cu 3d and Se 4p states in the valence band and an increase in the perturbation potential due to a lattice deformation.[29–31] Besides, according to the theoretical calculations of Jaffe and Zunger,[25] the upper valence band of Cu-III-VI_2 chalcopyrites is exclusively formed by the p-d hybridization of Cu 3d and VI 4p atomic levels. The strength of this $\Gamma_{15}(d)-\Gamma_{15}(p)$ interaction inversely depends on the energy separation between such levels. This repulsive interaction pushes the antibonding p-d states to higher energies; as a consequence, this effect produces a decrease in the band gap value.[14] In the case of Cu-poor CIS, the p-d repulsive interaction is expected to be smaller, lowering the VBM and inducing a smaller lowering in the CBM,[25,31] and hence, increasing the band gap value. On the other hand, our results show an increase in the band gap values of the Cu-poor samples compared to the stoichiometric ones, in both I35 and I58 series (Table II). After Han *et al.*[14,29,30] and according to the previous explanations, these results could be explained by the reduction in the p-d interaction.

The optical parameters of interest, namely, the complex refractive index $n^*=n+ik$, the normal-incidence reflectivity R, and the absorption coefficient α, can be readily computed from well known equations.[15,23]

Theoretical calculations of the electronic band structure

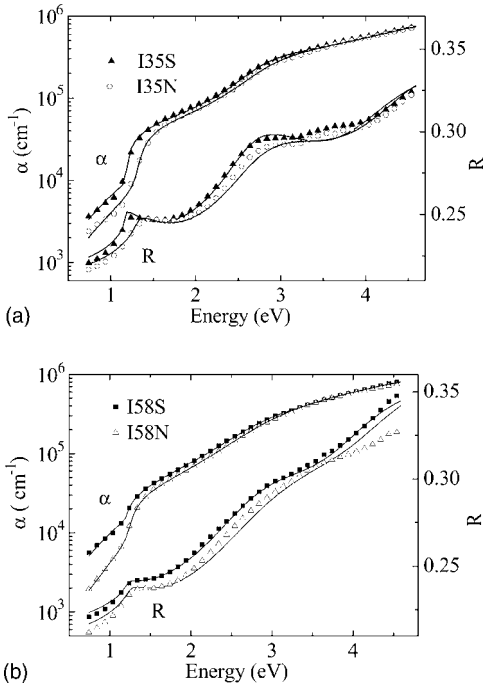

FIG. 2. Spectral dependence of the absorption coefficient (α) and normal-incidence reflectivity (R) for (a) I35 and (b) I58 samples. Experimental (triangles, circles, and squares) and theoretically calculated data using Adachi's model and the SA algorithm (solid lines) are also presented.

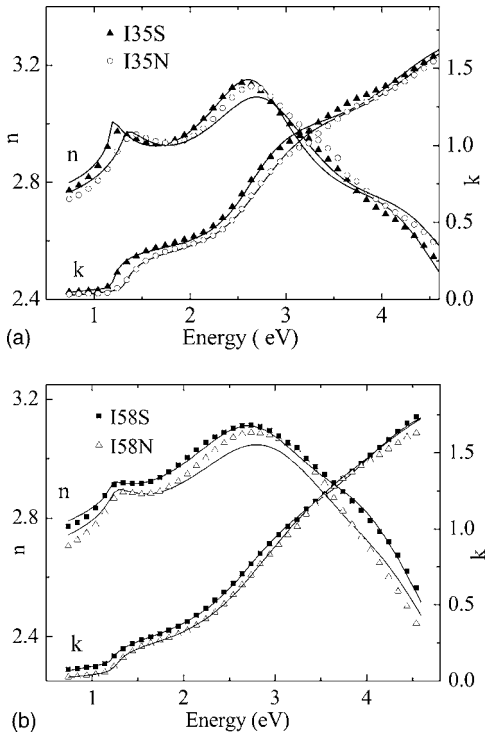

FIG. 3. Spectral dependence of the real refraction index (n) and extinction coefficient (k) for (a) I35 and (b) I58 samples. Experimental (triangles, circles, and squares) and theoretically calculated data using Adachi's model and the SA algorithm (solid lines) are also presented.

and the DOS for $CuInSe_2$ and $(4CuInSe_2)_y(CuIn_5Se_8)_{1-y}$ compounds show a reduction in the DOS within the 3–4 eV region from the VBM.[14,25,26,32] In addition, a reduction in the Cu 3d DOS near the VBM due to a Cu deficiency results in a decrease in the amplitude of the absorption coefficient α for CIS.[14] Therefore, a reduction in the experimental α values in Cu-deficient samples should be expected. The calculated and observed absorption coefficient spectra α are depicted in Fig. 2. The Cu-deficient $CuIn_5Se_8$ sample shows a depression of the absorption coefficient in the spectral region between 1 and 3 eV, which is in agreement with that observed in $(4CuInSe_2)_y(CuIn_5Se_8)_{1-y}$ films.[14]

The experimental spectral dependences of n and k, as well as the calculated ones using Adachi's model and the SA algorithm, are presented in Figs. 3(a) and 3(b) for $CuIn_3Se_5$ and $CuIn_5Se_8$ samples, respectively. A good agreement is observed for all of the studied samples, and the obtained values of the interband CP parameters (strength, threshold energy, and broadening) are given in Table II. All of these optical spectra were found to reveal distinct structures at these points.

The experimental n data have also been analyzed by using a simple theoretical model, namely, the first-order Sellmeier's equation as follows:[23]

$$n^2(\lambda) = A + \frac{\lambda^2}{\lambda^2 - B}, \tag{3}$$

where A and B are the fitting parameters, and λ is the wavelength of light in vacuum. The solid line in Fig. 4 represents the fitting of Eq. (3) to the experimental data. The values of the fitting parameters A, B are equal to 6.38, 0.63 and 6.45,

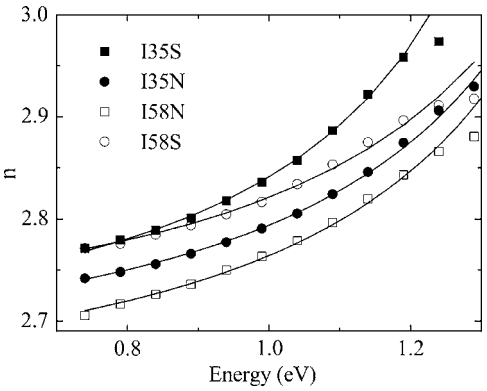

FIG. 4. n vs photon energy for I35S, I358N and I58S, I58N samples. The solid line shows the calculated result following Eq. (3).

0.52 for I35S and I58S nearly stoichiometric samples, respectively. The nonstoichiometric samples present the A, B values of 6.28, 0.53 and 6.11, 0.53 for I35N and I58N, respectively.

As $\lambda \to \infty$, the electronic contribution to the dielectric function approaches the limiting value ε_∞, i.e., the high-frequency dielectric constant. The value of $\varepsilon_\infty = n^2$ $(\lambda \to \infty) = A + 1$ is about 7.38–7.28 for $CuIn_3Se_5$ and 7.45–7.11 for $CuIn_5Se_8$. The reported values for $CuInSe_2$ and $CuGaSe_2$ ranged between 6 and 6.9 and between 4.2 and 5.1, respectively,[33,34] and that for $CuGa_3Se_5$ and $CuGa_5Se_8$ in the $\varepsilon_\infty = 7-7.2$ range.[23,28]

IV. CONCLUSIONS

The spectral dependence of the real, $\varepsilon_1(\omega)$, and imaginary, $\varepsilon_2(\omega)$, parts of the complex dielectric function, $\varepsilon(\omega)$, as well as of the complex refractive index, extinction and absorption coefficients, and the normal-incidence reflectivity for $CuIn_3Se_5$ and $CuIn_5Se_8$ crystals, is modeled in the 0.8–4.4 eV photon energy range by using a modification of Adachi's model for the optical properties of semiconductors and the SA algorithm. An excellent agreement with the experimental data has been obtained and the model parameters (strength, threshold energy, and broadening) have been determined. It has also been found that Cu-poor $CuIn_3Se_5$ and $CuIn_5Se_8$ samples show an increase in the band gap value probably due to a reduction in the p-d interaction at the valence band maximum. The present results offer a valuable set of optical-constant data for $CuIn_3Se_5$ and $CuIn_5Se_8$ that could be useful for the design of solar cells based on these compounds.

ACKNOWLEDGMENTS

Financial support from INTAS program (Project No. 03-51-6314), from Comunidad de Madrid government FOTOFLEX Project No. S-0505/ENE/0123, and from Spanish government MEC Project No. ENE 2004-07446-C02-01/ALT/ and No. MAT2003-01490 is acknowledged.

[1] K. Ramanathan, G. Teeter, J. Keane, and R. Noufi, Thin Solid Films **480–481**, 499 (2005).
[2] D. Schmid, M. Ruckh, F. Granwald, and H. W. Schock, J. Appl. Phys. **73**, 2902 (1993); L. Stolt, J. Hedstrom, J. Kessler, M. Puch, K. O. Velthaus,

and H. W. Schock, Appl. Phys. Lett. **62**, 597 (1993).
[3]H. Z. Xiao, L. Yang Chung, and A. Rockett, J. Appl. Phys. **76**, 1503 (1994).
[4]G. Marín, S. M. Wasim, C. Rincón, G. Sánchez-Pérez, Ch. Power, and A. E. Mora, J. Appl. Phys. **83**, 3364 (1998).
[5]C. Rincón, S. M. Wasim, G. Marín, and I. Molina, J. Appl. Phys. **93**, 780 (2003).
[6]A. J. Nelson, G. S. Horner, K. Sinha, and M. H. Bode, Appl. Phys. Lett. **64**, 3600 (1994).
[7]T. Negami, N. Kohara, M. Nishitani, T. Wada, and T. Hirao, Appl. Phys. Lett. **67**, 825 (1995).
[8]S. Mahanty, J. M. Merino, R. Díaz, F. Rueda, J. L. Martín de Vidales, and M. León, Inst. Phys. Conf. Ser. **152**, 499 (1998).
[9]C. Rincón, S. M. Wasim, G. Marín, R. Márquez, L. Nieves, G. Sánchez-Pérez, and E. Medina, J. Appl. Phys. **90**, 4423 (2001).
[10]L. Durán, C. Guerrero, E. Hernándes, J. M. Delgado, J. Contreras, S. M. Wasim, and C. A. Durante Rincón, J. Phys. Chem. Solids **64**, 1907 (2003).
[11]R. Bacewicz, J. Filipowicz, and A. Wolska, Inst. Phys. Conf. Ser. **152**, 507 (1998).
[12]I. V. Bodnar, I. T. Bodnar, V. F. Gremenok, A. M. Kovalchuk, and M. León, J. Cryst. Growth **293**, 324 (2006).
[13]S. Levcenko N. N. Syrbu, A. Nateprov, J. M. Merino, and M. León, J. Phys. D **39**, 1515 (2006).
[14]S.-H. Han, C. Persson, F. S. Hasoon, H. A. Al-Thani, A. M. Hermann, and D. H. Levi, Phys. Rev. B **74**, 085212 (2006).
[15]M. León, S. Levcenko, A. Nateprov, A. Nicorici, J. M. Merino, R. Serna, and E. Arushanov, J. Phys. D **40**, 740 (2007); M. León, R. Serna, S. Levcenko, A. Nateprov, A. Nicorici, J. M. Merino, and E. Arushanov, Phys. Status Solidi A **203**, 2913 (2006).
[16]M. I. Alonso, M. Garrida, C. A. Durante Rincon, and M. Leon, J. Appl. Phys. **88**, 5796 (2000); J. G. Albornoz, R. Serna, and M. Leon, *ibid.* **97**, 103515 (2005).
[17]R. M. A. Azzam and N. M. Bashara, *Ellipsometry and Polarized Light*, 1st ed. (North-Holland, Amsterdam, 1977).
[18]H. Y. Deng and N. Dai, Phys. Rev. B **73**, 113102 (2006).
[19]T. Kawashima, S. Adachi, H. Miyake, and K. Sugiyama, J. Appl. Phys. **84**, 5202 (1998).
[20]T. Kawashima, H. Yoshikawa, S. Adachi, S. Fuke, and K. Ohtsuka, J. Appl. Phys. **82**, 3528 (1997).
[21]A. B. Djurisic and E. Herbert Li, J. Appl. Phys. **85**, 2848 (1999).
[22]A. B. Djurisic and E. H. Li, Appl. Phys. A: Mater. Sci. Process. **73**, 189 (2001).
[23]M. León, R. Serna, S. Levcenko, A. Nateprov, A. Nicorici, J. M. Merino, and E. Arushanov, J. Appl. Phys. **101**, 013524 (2007).
[24]A. Corana, M. Marchesi, C. Martini, and S. Ridella, ACM Trans. Math. Softw. **13**, 262 (1987).
[25]J. E. Jaffe and A. Zunger, Phys. Rev. B **28**, 5822 (1983).
[26]F. Jiang and J. Feng, Appl. Phys. Lett. **89**, 221920 (2006).
[27]M. I. Alonso, K. Wakita, J. Pascual, M. Garriga, and N. Yamamoto, Phys. Rev. B **63**, 075203 (2001).
[28]M. León, S. Levcenko, A. Nateprov, J. M. Merino, E. J. Friedrich, R. Serna, and E. Arushanov, J. Appl. Phys. **102**, 113503 (2007).
[29]S.-H. Han, A. M. Hermann, F. S. Hasoon, H. A. Al-Thani, and D. H. Levi, Appl. Phys. Lett. **85**, 576 (2004).
[30]S.-H. Han, F. S. Hasoon, J. W. Pankow, A. M. Hermann, and D. H. Levi, Appl. Phys. Lett. **87**, 151904 (2005).
[31]M. León, J. M. Merino, and E. Arushanov, Moldavian J. Phys. Sci. **5**, 373 (2006); M. León, J. M. Merino, and E. Arushanov, Third International Conference on Materials Science and Condensed Matter Physics, MSCMP, Chisinau, 2006.
[32]S. B. Zhang, S.-H. Wei, A. Zunger, and H. Katayama-Yoshida, Phys. Rev. B **57**, 9642 (1998).
[33]C. Domain, S. Laribi, S. Taunier, and J. F. Guillemoles, J. Phys. Chem. Solids **64**, 1657 (2003).
[34]N. N. Syrbu, M. Bogdanash, V. E. Tezlevan, and I. Mushcutariu, Physica B (Amsterdam) **229**, 199 (1997).